On a Possible Approach to Risk Prediction of Recurrence of Atrial Fibrillation after Catheter Ablation According to Data from the Pre-procedure Period

Iskren Garvanski[1,2], Mikhail Matveev[1*], Vessela Krasteva[1], Todor Stoyanov[1], Iana Simova[3]

[1]*Institute of Biophysics and Biomedical Engineering*
Bulgarian Academy of Science
Acad. G. Bonchev Str., Bl. 105, 1113 Sofia, Bulgaria
E-mails:mgm@biomed.bas.bg, vessika@biomed.bas.bg,
tstoyanov72@gmail.com

[2]*Acibadem City Clinic Cardiovascular Center*
127 Okolovrasten pat, 1700 Sofia, Bulgaria
E-mails: i.garvanski@gmail.com

[3]*Heart and Brain Center of Excellence, University Hospital Pleven*
2 Pier Curie Str.,5804 Pleven, Bulgaria
E-mail: ianahr@ yahoo.com

[*]*Corresponding author*

Received: June 23, 2021 **Accepted: February 03, 2022**

Published: March 31, 2022

Abstract: *The aim of the study is to identify and evaluate predictors of recurrent paroxysms of atrial fibrillation (AF) paroxysms based on data from the preprocedural period among personal indices, history, comorbidities, ultrasound examination, and morphological components of f-waves, such as spectral amplitude and frequency. 39 patients with antral pulmonary vein isolation using radiofrequency or cryoenergy were included. Spectral analysis of f-waves was performed by fast Fourier transform of the ECG signal after suppression of the T-wave and QRS-complex. The performed U-test for the difference between the amplitude and frequency indicators in the groups without and with recurrence of AF shows a significant difference between the amplitude values in the two studied groups of patients. Through a stepwise discriminant analysis of a total of 14 indicators, 5 reliably separated groups without and with recurrence were determined: Echo LV-EF, spectral amplitude of f-waves, heart failure, Stroke/TIA, diabetes. The discriminator synthesized on these indices classified among the 39 patient – 25 without relapse (group 1) and 14 with relapse (group 2), 3 patients wrong from group 1 to group 2 (false positive), or 12%, and 1 patient was wrong from group 2 to group 1 (false negative), or 7.1%. These results give grounds to accept the hypothesis that it is possible to develop a decision rule for determining the degree of risk of post-procedural recurrence of AF from pre-procedural period data.*

Keywords: *Atrial fibrillation, Catheter Ablation, Post-procedural recurrence of atrial, Fibrillation.*

Introduction

Atrial fibrillation (AF) is the most common clinically manifested arrhythmia in the developed world, with one in four middle-aged individuals in Europe and the USA developing AF [8]. Although with no immediate risk to the patient's life, atrial fibrillation leads to an increased risk of embolic events and ischemic stroke. AF is one of the causes of manifestations of heart

failure, impaired quality of life, cognitive dysfunction and depression [12]. Restoration and maintenance of sinus rhythm is a key therapeutic goal in patients with AF.

Since the introduction of the transcatheter ablation technique in 1998, the technology and technique for performing the procedure have evolved considerably, and catheter ablation (CA) is currently used with high a class of indications to improve symptomatology in cases of paroxysmal AF in symptomatic patients, in whom antiarrhythmic therapy is ineffective. The superiority of CA over antiarrhythmic therapy has been demonstrated in large randomized trials. From the CABANA (Catheter Ablation vs. Anti-arrhythmic Drug Therapy for Atrial Fibrillation Trial) [14], which compared drug therapy versus pulmonary vein isolation in patients with AF, it appears that the initial postprocedural success rate of pulmonary vein isolation in AF is high, but the long-term efficacy of the procedure remains a challenge, thus finding predictors of procedure success is of great importance.

Several predictors of recurrence have been identified in various studies. In a publication, Sultan et al. [20] described several statistically significant predictors of AF recurrence after ablation, based on data from 3703 patients undergoing treatment for AF at 40 German centers, with a mean follow-up of 463 days. The data suggest that the clinical type of AF, comorbidities such as impaired renal and cardiac function, are strong predictors of AF recurrence.

Several echocardiographic parameters have been evaluated as a predictor of AF recurrence. In a literature review by Liżewska-Springer et al. [10], twenty-one articles were analysed and several characteristics were outlined. Left atrial diameter, right atrial size, indexed right atrial volume, left ventricular ejection fraction, and diastolic dysfunction had a significant preprocedural predictive value and outlined borderline values as indices predicting a higher incidence of AF recurrence after ablation. The presence of left ventricular (LV) systolic dysfunction also decreased the success rate of the procedure.

The concept of pulmonary vein volume, measured by computed tomography as a predictor of AF recurrence, was investigated by Shimamoto et al. [18]. The study demonstrated that larger total pulmonary vein volume and ostial pulmonary vein area were associated with AF recurrence after radiofrequency catheter ablation (RFA).

In addition to clinical and imaging characteristics, electrocardiographic (ECG) characteristics have also been analysed as a predictor of AF recurrence. Electrocardiographic findings in AF are characterized by the absence of P-waves on the cardiogram, an irregular R-R interval, and the presence of small fibrillation waves called f-waves. It is the f-waves that reflect atrial activity giving rise to AF [16]. The question of whether the morphology of these waves could predict atrial remodeling has been thoroughly investigated. For example, low-amplitude f-waves in leads aVF and V1 have been shown to be associated with late AF recurrence after ablation. On ECG, the amplitude of f-waves depends on the magnitude of the baseline voltage, which is related to the size of the remaining viable atrial myocardium, hence to the substrate for arrhythmia [4].

Since f-waves are a natural marker of AF in the ECG, it is natural to study their morphological features in more detail as possible predictors of recurrence after ablation. According to Park et al. [15], f-wave amplitude can be used to differentiate patients with long-standing persistent AF from other AF groups. The use of more than one lead has been proposed to increase predictive ability, with the simultaneous use of I, V1, V2, V5 showing the highest ability [23]. A publication by Nault et al. [13] reported that high f-wave amplitude

calculated from V1 was a predictor of intraprocedural arrhythmia termination in patients with persistent AF, as well as of maintenance of sinus rhythm at 12 months follow-up. The measurement of the amplitude of the f-waves in the publication is done manually, which implies large deviations depending on the respective researcher.

These features, as well as the importance of electrocardiographic analysis in patients with AF, determine the need for a more detailed study of the prognostic value of morphological features of f-waves in patients with AF in the preprocedural period – spectral amplitude and frequency.

In this study, we aimed to identify and evaluate predictors of recurrent AF paroxysms, using data from the preprocedural period among personal indices, history, comorbidities, ultrasound examination, and morphological components of f-waves, such as spectral amplitude and frequency.

Materials and methods

Patient collective

A total of 39 patients were included in the follow-up, of whom 30 were men (76.9%) and 9 were women (23.1%). The mean age of the participants was 61 years (± 6.94; 48-74). The mean body mass index in the study population was 29.9 (± 4.88). Paroxysmal AF was the most common clinical form of AF in 24 patients (61.5%), 10 patients had persistent AF (25.6%), and 5 patients had the procedure against the background of long-standing persistent AF (12.8%). The mean CHADS VASc score [6] in the study group was 2 (± 1.36). Thirty-three (84.6%) of the patients were found to have concomitant arterial hypertension, 8 (20.5%) patients had concomitant diabetes mellitus, and 4 (10.25%) patients were diagnosed with heart failure at the time of initiation of follow-up, and we considered patients with manifestations of heart failure on the background of reduced ejection fraction and those with moderately reduced ejection fraction, i.e., six (15.4%) patients had known ischemic heart disease, and 1 (2.56%) patient had undergone bypass surgery in the past. For patients with ischemic heart disease, we considered those with known coronary stenosis objectified by imaging or those with coronary revascularization. Of the group of patients, 1 (2.56%) had a history of rheumatic disease and 2 (5.12%) had moderate mitral insufficiency.

Patients in the formed database meet the following inclusion and exclusion criteria:

Inclusion criteria

- Paroxysmal, persistent or long-standing persistent AF documented by 12-lead ECG.
- High symptomatic class at the time of seizures, with EHRA IIB as a minimum for inclusion in follow-up.
- Ability to record an electrocardiogram during a seizure.
- Patients undergoing antiarrhythmic therapy with AF recurrences on background therapy.
- Patients suitable for ablation according to the current recommendations of the European Society of Cardiology [12].
- Ages 18 to 75.

Exclusion criteria

- Asymptomatic AF.
- Presence of a reversible cause of AF (endocrine disease; recent surgery; seizure due to alcohol intoxication, acute coronary syndrome).
- Previous ablations or MAZE procedure on the occasion of AF.

- High functional class heart failure (NYHA IV) or high functional class angina (CCS III-IV).
- Comorbidities with life expectancy less than 1 year.
- Unwillingness or contraindication to take anticoagulant therapy.
- History of heparin-induced thrombocytopenia.

In all patients, antral pulmonary vein isolation (PVI) was performed using radiofrequency or cryo energy, with additional lesions in the left and right atrium (LA; RA) at the operator's discretion. An irrigated ablation catheter was used for RFA and a dedicated cryoballoon was used for cryoablation.

A high power-short duration (HPSD) protocol was used in RFA, while controlling the lesions performed by ablation index. The ablation index is a numerical value, derived from the catheter contact force, energy and ablation time. The target for lesions was an ablation index of 500 on the anterior wall of the LP and 400 on the posterior wall. The energy used was 50 watts in all zones, irrigation rate 17 ml/min during ablation with a target contact force of 10 g. Point applications were marked on the three-dimensional anatomical map as points on the surface or as three-dimensional spheres with a diameter of 6 mm.

The high energy, short duration lesion approach, guided by an ablation index, was based on the FAFA study protocol [3].

Processing of ECG signals for spectral analysis of f-waves

A personal computer ECG system was used [19]. The system receives the signals from all electrodes synchronously through an additional isolated amplifier. It removes the network interference and suppresses the zero line drift, presents the recorded signal in real time on the screen. Received signals are recorded into the computer's memory and, after the recording is complete, saved to the hard disk for further processing and analysis. The system has the capability of real-time visualization of the standard 12 ECG leads. The signal is recorded in its original form, i.e., raw, for further processing and analysis outside real time.

The computer system has the following characteristics:

- synchronous recording of selected leads (up to 12 leads), with high frequency sampling (up to 2 kHz);
- real-time ECG signal display with network interference filtering and suppressed zero line drift;
- outside real time, the recorded signals are processed and reviewed and QRS detection is performed.

The system consists of two modules: an external isolated amplifier (for electrical safety), and a receiving part – a personal computer with specialized software. The connection between the two modules is made using a USB port. The isolated module operates at a preset sampling rate (up to 2 kHz), with a resolution of 24 bits per channel, which is provided by a 24-bit multi-channel analog-to-digital converter. Actions to obtain frequency spectra of ECG recordings, taken before ablation of patients, were performed in the following sequence (procedures were developed in a Matlab 2016 environment (Mathworks Inc.)):

1. Read signals from the database that are registered in multichannel format, with a sampling rate of 2 kHz and an amplitude resolution of 0.047684 μV (24-bit analog-to-digital conversion with a dynamic range of 800 mV).

2. Pre-processing of ECG signals, which includes:
   2.1. Calculation of the leads of a standard 12-lead ECG from the baseline 8: {I, II, III = II-I, avR = – (I + II)/2, avL = I-II/2, avF = II-I/2, V1, V2, V3, V4, V5, V6}.
   2.2. Reduce the sampling rate from 2000 Hz to 500 Hz, by taking 1 out of every 4 consecutive readings.
   2.3. Selection of a representative segment for analysis with a duration of 60 s, in a low-noise section of the recording. Visual evaluation of the entire recording is applied, and the selected segment includes a section in which there is no signal loss or saturation in any of the channels, no large dynamic amplitude changes due to motion artifacts, or no zero-line drift. This preselection is made to ensure an input signal that would minimize parasitic components in the spectrum from external sources unrelated to cardiac activity.
   2.4. Selection of a representative lead applying a criterion of high amplitude of visible atrial waves.
   2.5. Eliminate the constant (DC) offset of the entire ECG signal by linearly subtracting the point amplitude from the isoelectric line calculated for each lead at the beginning of the recording.
   2.6. Network interference filtering (50 Hz) by averaging filter (moving averaging) (averages 10 points, covering one period of network interference at a sampling rate of 500 Hz).
   2.7. A low-pass 1st order Butterworth filter with a cutoff frequency of 150 Hz, which was chosen according to the accepted convention for the upper cutoff frequency in diagnostic ECG analysis (International Electrotechnical Commission (IEC) Standard) [7].
   2.8. *For the QRS detector*: a 1st order high-pass Butterworth filter with a cutoff frequency of 2 Hz, which is selected with a high cutoff frequency adopted in monitoring ECG systems operating in high drift conditions. Such a filter provides higher noise immunity of the QRS detector.
   2.9. *For frequency analysis*: a 1st order high-pass Butterworth filter with a cutoff frequency of 0.1 Hz, in order not to filter out low-pass components, which are the subject of analysis in this work.
3. QRS detection applied to the selected representative lead.
   3.1. The QRS detector was implemented according to the procedure described in reference [5, 22]. It was developed for real-time systems, where the amplitudes of the recorded successive ECG signal discretes are compared with three thresholds, calculated based on maximum positive amplitude, maximum negative amplitude and maximum slope within a previous RR interval. The amplitude and slope thresholds are dynamic, and they decrease nonlinearly with a certain adaptation factor from a maximum to a minimum level, following the probability with which a new QRS-complex is expected to occur. The principle of dynamic threshold change and the criteria for QRS detection have been optimized in [5, 22]. There, the high sensitivity and accuracy of the positive prediction of the QRS detector (about 99.6%) has been demonstrated and tested on public databases (AHA, MIT-BIH Arrhythmia, European ST-T).
   3.2. The QRS detector makes a decision to locate the point of the QRS-complex with the highest (in absolute value) amplitude (called Rpeak below). The maximum amplitude is considered as an indicative benchmark that ensures synchronous registration of

consecutive QRS-complexes in the same area of the complex (at the same time within a cardiac cycle). The purpose of this approach is to avoid fluctuation of RR intervals resulting from non-synchronous detection in different areas of the QRS-complex (phase offset).

4. Synthesis and measurement of waves in a synchronously averaged complex:
   4.1. Calculation of a mean heart rate (HR), reflecting the mean RR-interval within the analysed representative segment:
   HR = 60Fs/mean(RR(i)), where:
   i = 1, 2, ..., N – 1, with N is the number of RR-intervals;
   RR(i) = Rpeak(i + 1) – Rpeak(i) is the value of the i^{th} RR-interval;
   Fs = 500 Hz is the sampling frequency.
   4.2. Separation of windows around each recorded QRS-complex with width BeatWindow = [Rpeak – 150 ms; Rpeak + minRR], where Rpeak is the point of recorded peak of QRS-complex, minRR is the minimum RR-interval recorded within the analyzed representative segment. The windows are synchronous for all leads, using Rpeak on the representative lead as a benchmark.
   4.3. Averaging all windows within the analysed representative segment and computing a synchronously averaged complex for each outflow:
   AverageBeat = sum(BeatWindow)/N
   4.4 Detection of Q, J points for the beginning and end of QRS on the averaged complex of each lead by the method of Christov and Simova [5], which is distinguished by high accuracy.
   4.5. Detection of Q, J, T-end points for the QRS start and end and T-wave end on the averaged complex of each lead by the method of Christov and Simova [5].
   4.6. Resetting the averaged complex of each lead during the low-amplitude section of the TQ interval, as shown in Fig. 1. The goal is not to average a signal during the isoelectric loop representative of atrial activity.

5. Synthesizing ECG signal for frequency analysis:
   5.1. T-wave suppression in the input ECG signal by subtracting the averaged AverageBeat complex (in the section after the J-point) from each recorded QRS complex, as shown in Fig. 2. The synchronization between AverageBeat and QRS complexes follows the concept of Rpeak alignment of the representative lead. The subtraction of AverageBeat from the input signal is done separately for each lead.
   5.2. Suppression of the QRS-complex in the input ECG signal by linear interpolation of the amplitudes between the beginning and the end of each recorded QRS-complex, as shown in Fig. 3. The times measured for the Q and J points on the averaged complex are used as the start and end of each recorded QRS-complex. The procedure is applied independently with the Q and J measurements for each lead.
   5.3. Frequency analysis by fast Fourier transformation of the ECG signal after T-wave and QRS-complex suppression. The Matlab library function fft(ECG) was applied and all points of the input signal were passed to it. The amplitude-frequency spectrum was analysed.

Statistical methods used. Classification of patients with and without AF recurrence after CA, according to data from the preprocedural period. Stepwise linear discriminant analysis.

Statistical estimates for indicators from descriptive statistics were used in the study. We used the non-parametric **Mann-Whitney U-test** to compare two samples of variable values **because it is applied when the samples have small and different numbers of data and do**

not follow a normal distribution. In our study, the qualitative variable for comparison was the presence/absence of AF recurrence after ablation; the quantitative variables were the values of the spectral characteristics of the f-waves (amplitude and frequency) and data from the included patients' clinical preprocedural parameters. For the distributions of parameters analysed by histograms, the theoretical normal distributions for the obtained statistics were calculated using the Kolmogorov-Smirnov test.

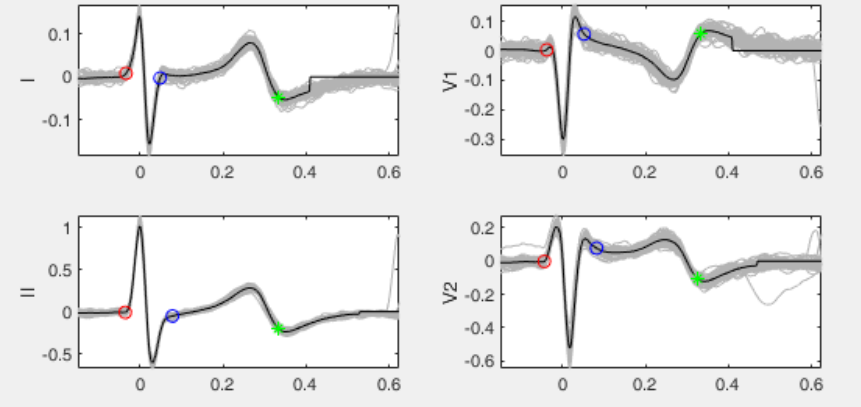

Fig. 1 Detection examples of Q(o), J(o) and Tend(*) points on the averaged complex (black line) of different leads. Shown is the strategy for resetting the averaged complex in a low-amplitude section after the end of the T-wave, in which predominantly atrial activity is expected to be visible.

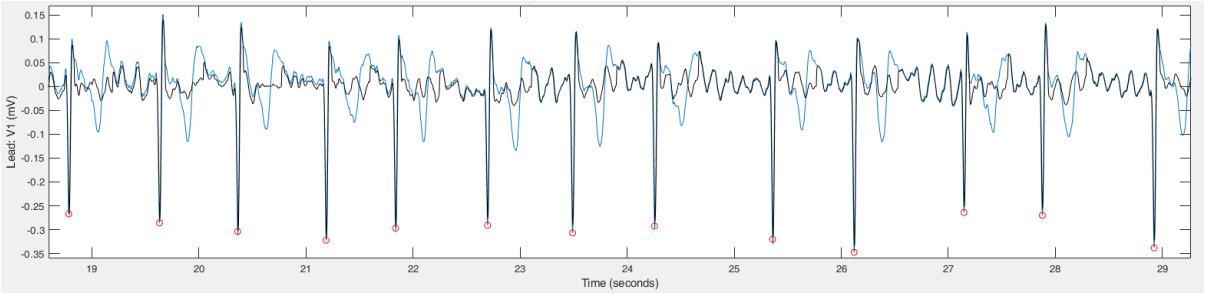

Fig. 2 Example of T-wave suppression by subtraction of an averaged complex (after the J -point). In the figure, Rpeak(o) are labelled, which are used to synchronize the averaged complex.

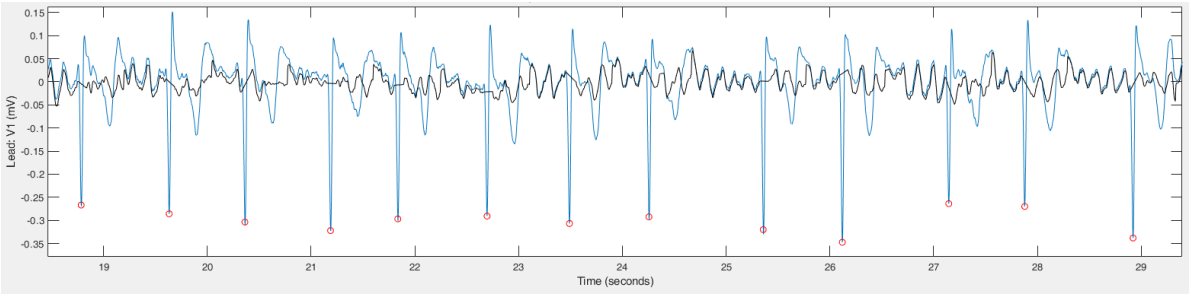

Fig. 3 The signal from Fig. 2, on which the QRS-complexes were further suppressed by linear interpolation between the origins and termini of all QRS-complexes, using the measured Q and J times of the averaged complex

Discriminant analysis (DA) [9] is a statistical method designed to study differences between two or more groups of objects using data on the diversity of several attributes that distinguish these objects from each other. A typical task of discriminant analysis is to identify those features that best discriminate between objects belonging to different groups. We used stepwise discriminant analysis (SDA) to create a model that allowed the most complete discrimination between the two data sets, comprising of patients with and without AF recurrences after ablation.

The reasons to use DA were:

- ***to determine, on the basis of the available data, a constellation of indicators that are informative for the correct classification of patients into the two groups;***
- ***to establish the involvement of the spectral indices of f-waves in this constellation, as well as their weight among the other indicators in the constellation.***

For statistical data analysis and classification procedure, we used the Statistica 7 vs. statistical package from StatSoft, Inc. In the statistical procedures we used, the criterion for the reliability of the conclusions everywhere was assumed to be a probability level of $P = 0.95$ (95%) (or, equivalently, a confidence level of $p = 0.05$).

Results

Patient collective data from the pre-procedure period and data on recurrences

In Table 1, the data from the pre-procedure period are included among personal indicators, history, comorbidities, ultrasound examination, and data on recurrences of AF until the 3rd, 6th and 12th month post-procedure.

Amplitude-frequency analysis of the f-waves in the studied groups

We present the results of the successive processing steps and amplitude-frequency analysis of the *f-waves* in the group without recurrence after CA (25 subjects), and in the group with recurrence in the period of 12 months after the procedure (14 subjects), respectively, with one typical case from each of the two groups.

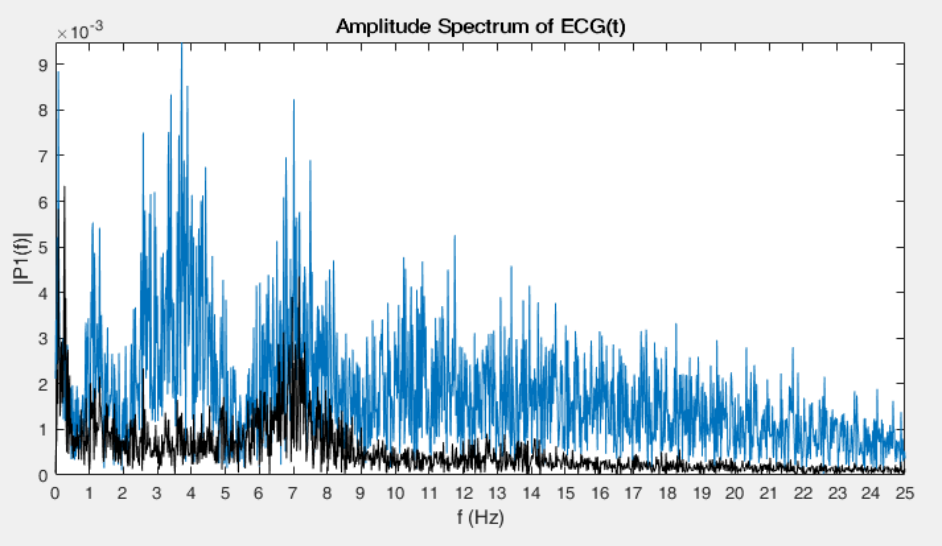

Fig. 4 Example of ECG signal amplitude spectrum before (blue) and after (black) application of the T-wave and QRS-complex suppression method

Table 1. Patient data from the study subjects

From	1: male / 2: female	Date of procedure	procedure	Age	Height	Weight	BMI	Hx of AF [yrs]	Hypertension (1 / 0)	Diabetes	Stroke / TIA	Heart failure	Coronary heart disease	Chads-vasc score	Other cardiac disease	Echo LA diameter	Echo LV-EF	Current AADs (class)	AF at 3 months	AF at 6 months	AF at 12 months
1	**1**	11.4.2018	PVI + CS + MI	54	190	120	33	3	0	0	0	0	0	0	0	47	42	III	0	0	0
2	**1**	23.5.2018	PRS	67	190	110	30	1	1	0	0	0	0	2	0	43	54	III	1	1	1
3	**1**	11.7.2018	PVI + MI + post + inf	44	190	124	34	5	1	0	0	0	0	1	modern MI	42	51	III	0	0	0
4	**1**	08.8.2018	PVI + roofline + RA	67				1	1	1	1	0	0	5	0	60	56	III	0	0	0
5	**1**	23.10.2018	PRS	67	176	86	28	3	1	1		1	1	5	ICM; VT; ICD	49	33	III	0	0	0
6	**1**	27.9.2018	PVI + Roofline + RPV anterior + inf	57	176	110	35	11	1	0	0	0	0	1	modern MI	44	65	III	1	n/a	n/a
7	**1**	10.10.2018	PRS	57	183	97	29	25	1	0	0	0	0	1		40	70	III	0	0	0
8	**1**	16.10.2018	PRS	58	170	90	31	2	1	1	0	0	0	2	ASD II type	50	61	III	0	1	1
9	**1**	08.3.2019	PRS + CTI	61	176	107	35	2	1	0	0	0	0	1		44	55	IC	0	0	0
10	**1**	29.1.2019	PVI + CS	58	186	90	26	1	1	0	0	0	0	1		47	70	IC	1	1	1
11	**2**	29.1.2019	PRS	60	160	85	33	8	1	0	0	0	0	2		38	52	III	0	0	0
12	**1**	11.2.2019	PRS	48	185	90	26	2	0	0	0	0	0	0		42	59	III	0	n/a	0
13	**1**	19.2.2019	PVI + Roofline + mitral isthmus	66	176	90	29	9	1	1	1	0	0	5		47	68	III	0	0	0
14	**1**	26.2.2019	PVI + roofline	66	170	93	32	4	1	0	0	0	0	2		43	67	III	0	0	0
15	**1**	26.2.2019	PVI + mitral isthmus + posterior	58	177	137	44	12	1	1	0	0	0	2		56	62	III	0	1	0
16	**1**	11.3.2019	PVI + CS + CFAE	68	178	78	25	1	1	0	0	0	0	2		45	55	III	0	n/a	n/a
17	**1**	02.4.2019	PRS	72	183	100	30	2	1	0	0	0	1	3		43	63	III	0	0	
18	**1**	09.4.2019	PVI + postinf	54	180	120	37	3	1	0	0	0	0	1		60	54	III	0	0	0
19	**2**	23.4.2019	PRS	63	164	97	36	5	1	1	0	0	0	3		40	61	III	1	1	1
20	**2**	19.9.2019	PRS	58	163	63	24	2	1	0	0	0	0	2		45	61	III	0	0	0

21	**1**	03.10.2019	PRS	71	173	84	28	1	1	0	1	1	0	4	modern MI	54	54	iC	1	1	1
22	**1**	19.10.2019	PVI + CS + CFAE	53	179	71	22	6	0	0	0	0	0	0		45	62	III	1	1	1
23	**1**	19.10.2019	PRS	64					1	0	0	1	0	2	AVR / MVR	38	53	III	0	0	
24	**2**	21.10.2019	PRS	70	172	75	25	1	0	0	0	0	0	2		40	50	III	0	0	
25	**2**	29.11.2019	PRS	58	170	80	28	1	1	0	0	0	0	2		40	65	III	1	1	1
26	**1**	30.11.2019	PRS	53	180	82	25	1	0	0	1	0	0	2		35	55	III	0	0	1
27	**1**	30.11.2019	PRS	65	173	100	33	2	1	0	0	1	1	4		50	38	III	0	1	
28	**1**	02.12.2019	PRS	64	175	112	37	10	1	0	0	0	0	1		48	65	III	0	0	0
29	**2**	02.12.2019	PRS	66	171	88	30	15	1	0	0	0	0	3		45	68	III	0	1	1
30	**1**	06.12.2019	PRS	51	180	90	28	1	1	0	0	0	0	1		43	50	III	0	0	0
31	**1**	07.12.2019	PRS	63	172	70	24	1	1	0	0	0	0	1		40	61	III	0	0	1
32	**1**	07.12.2019	PRS	74	170	70	25	2	1	1	0	0	1	4		44	45	III	0	0	0
33	**1**	02.1.2020	PRS	52	185	88	26	1	1	0	0	0	0	1		43	65	III	0	1	1
34	**1**	20.1.2020	PRS	60	179	90	28	3	1	0	0	0	1	2		42	54	III	0	0	0
35	**2**	23.1.2020	PRS	65	163	63	24	2	1	0	0	0	0	3		44	61	III	0	0	0
36	**2**	27.1.2020	PRS	72	163	92	34	3	1	0	0	0	0	3		43	52	III	0	0	0
37	**1**	12.3.2020	PRS	55	180	90	27	4	0	0	0	0	0	0		40	59	III	0	0	0
38	**1**	12.3.2020	PRS	58	176	118	38	3	1	0	0	0	1	1	ACB x3	44	57	III	0	0	0
39	**2**	13.3.2020	PRS	64	165			4	1	1	0	0	0	1	Rheumatism	44	60	III	0	0	0


ECGFTDPrg
File Actions Leads COM Port Speed Info
Vertical Zoom
Horizontal Zoom
ECG Mode
ECG Zoom
DrvLeg
Crc Errors
Frm Cnt Errors
Power line Filter
Disabel Alarm Msg
Custom Parameters
Patinet Info
I
II
III
aVR
aVL
aVF
V1
V2
V3
V4
V5
V6

a)

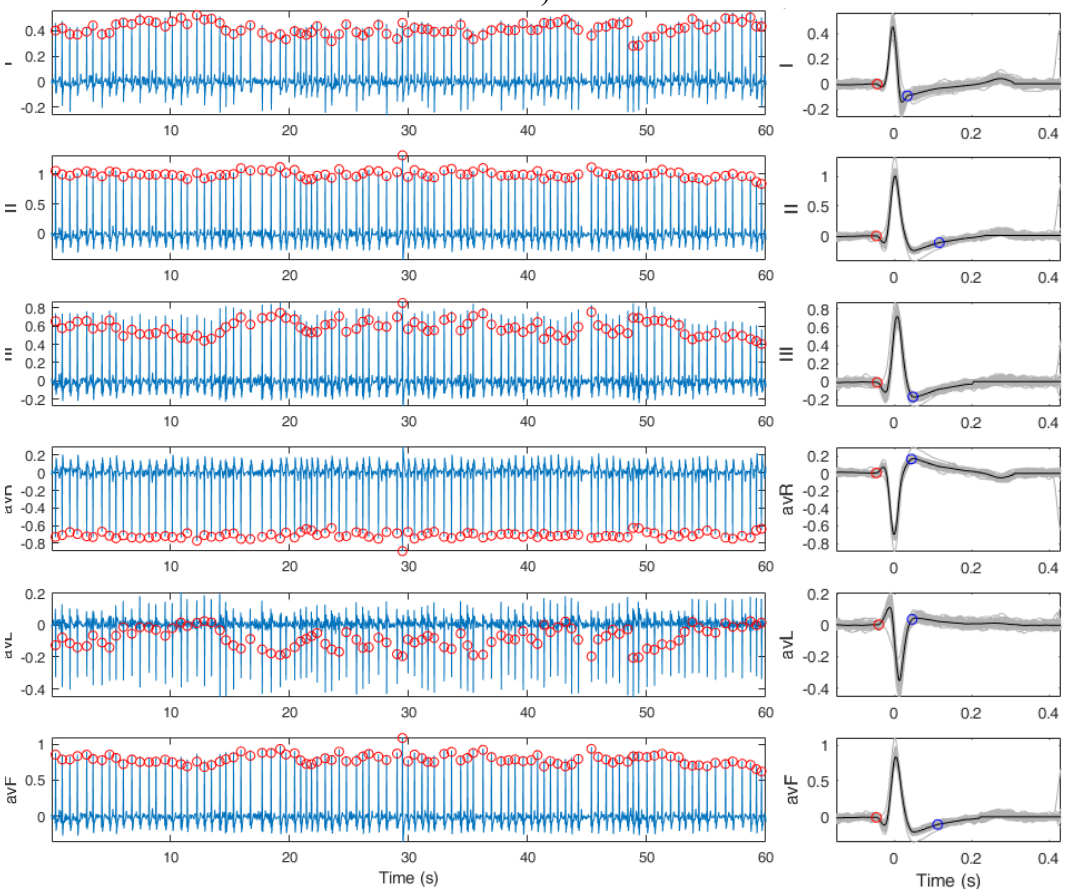
I
II
III
avR
avL
avF
Time (s)
Time (s)

b)

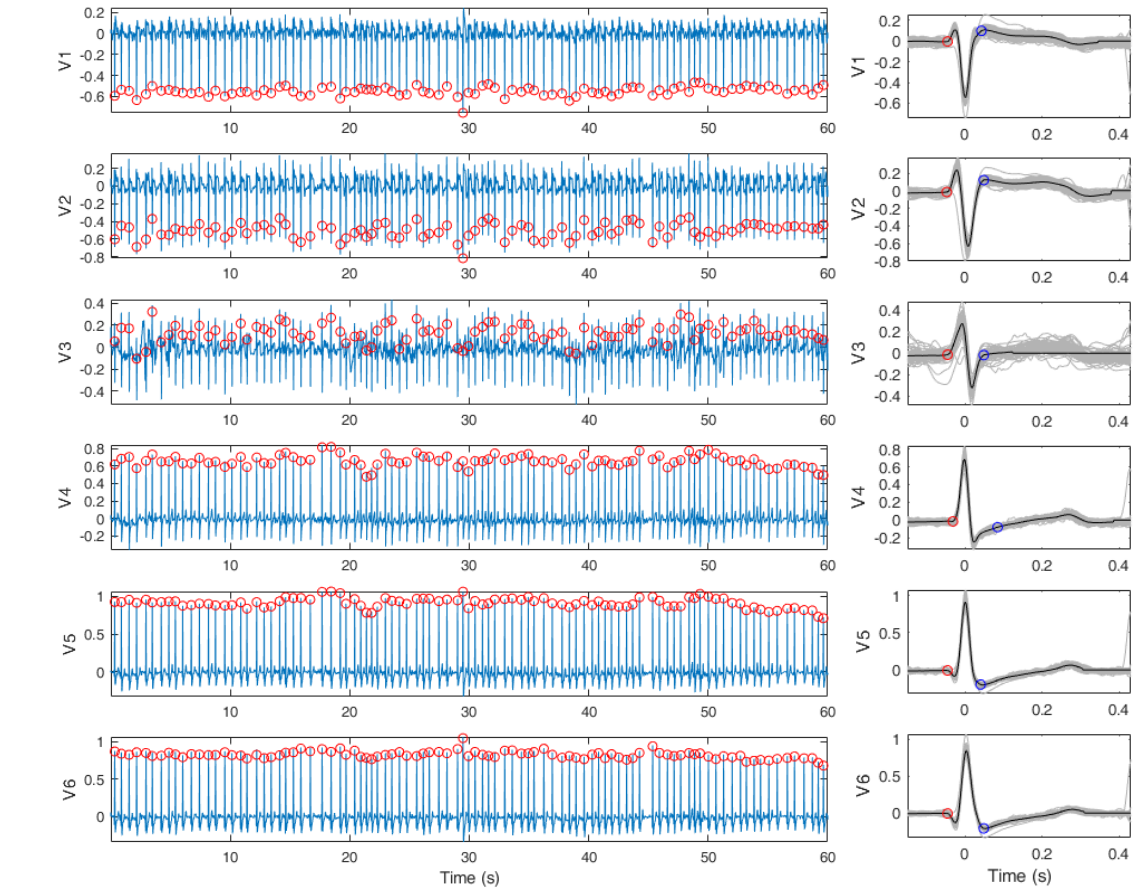

c)

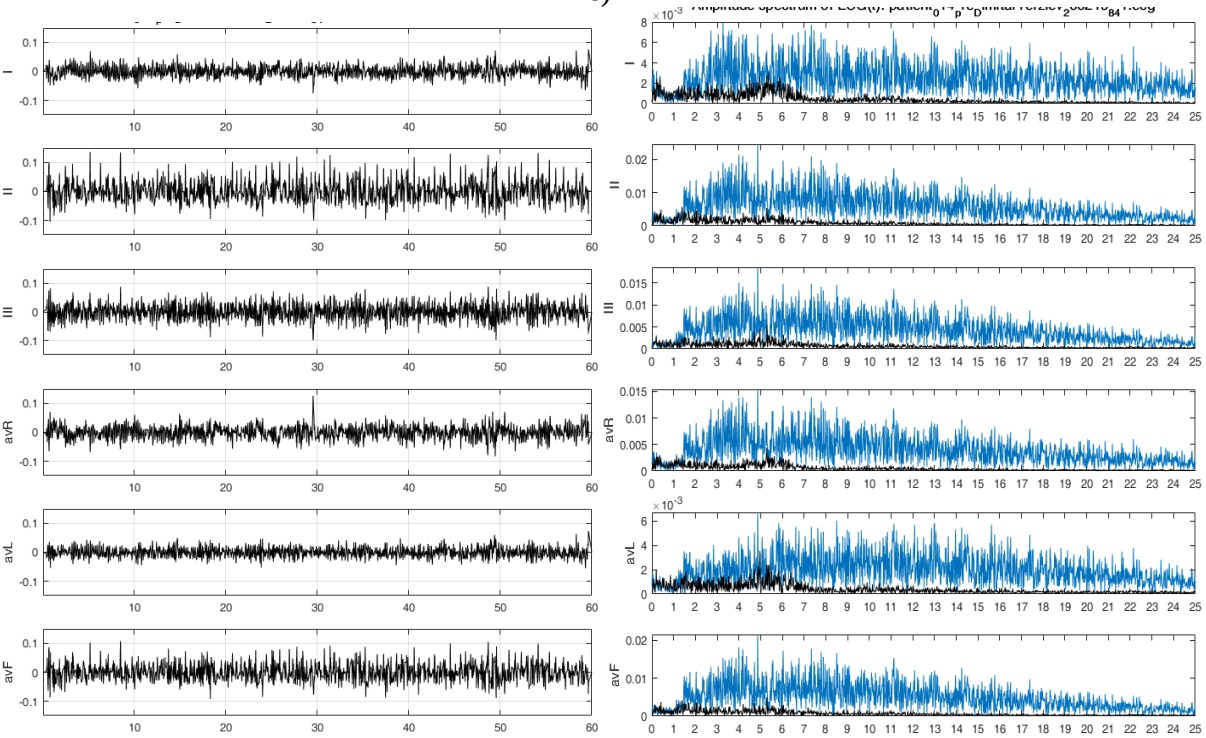

d)

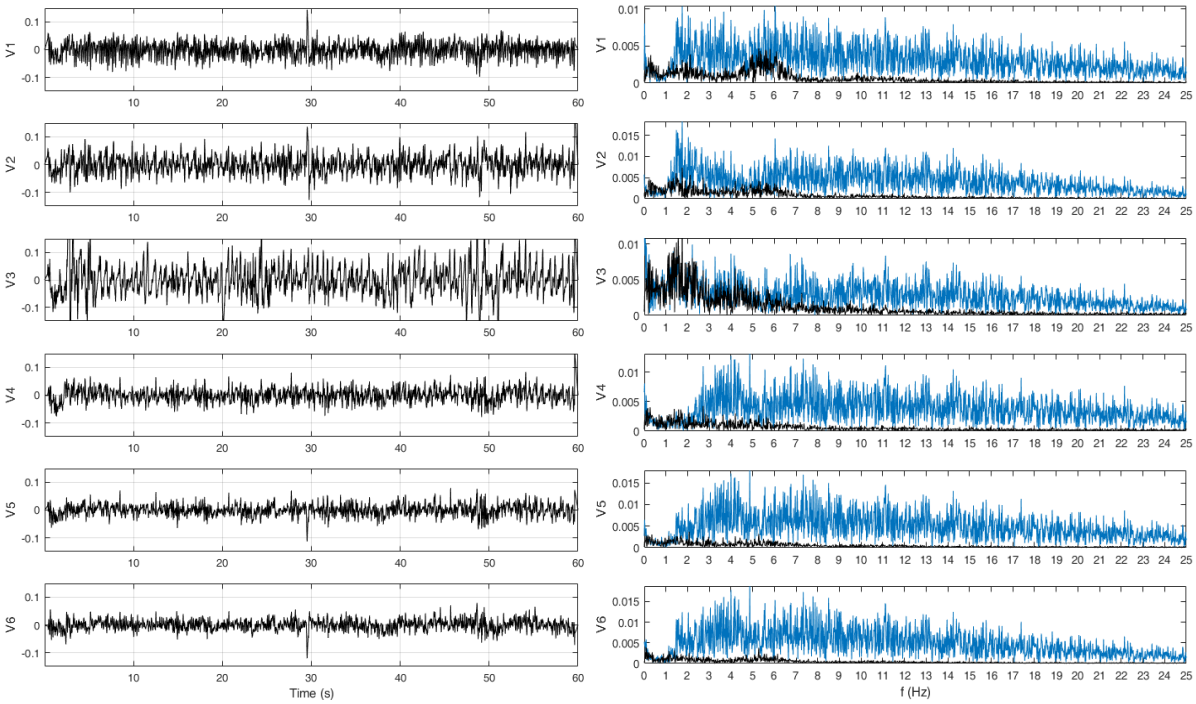

e)

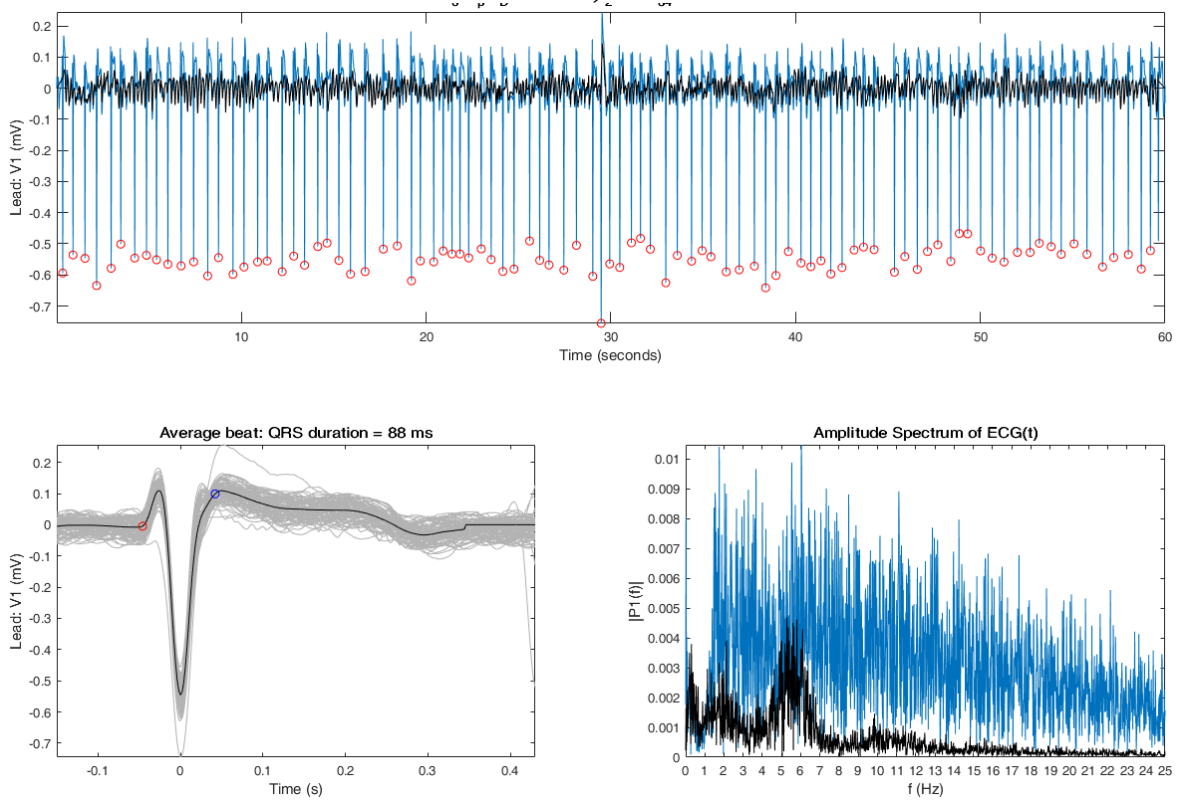

f)

Fig. 5 Sequential procedures for obtaining the amplitude-frequency spectrum by ECG registration for patient No. 14 of the group without AF recurrence postprocedurally: the original signal; the signal in the 12 leads with detected QRS-complex (left) and averaged QRS-complex in each lead; the signal after extraction of the averaged QRS-T segment; the amplitude-frequency spectra of the signal for each lead after extraction; the indicated procedures for the lead selected as representative lead V1.


ECGFTDPrg
File Actions Leads COM Port Speed Info
Vertical Zoom
Horizontal Zoom
ECG Mode
ECG Zoom
DrvLeg
Crc Errors
Frm Cnt Errors
Power line Filter
Disabel Alarm Msg
Custom Parameters
Patinet Info
I
II
III
aVR
aVL
aVF
V1
V2
V3
V4
V5
V6

a)

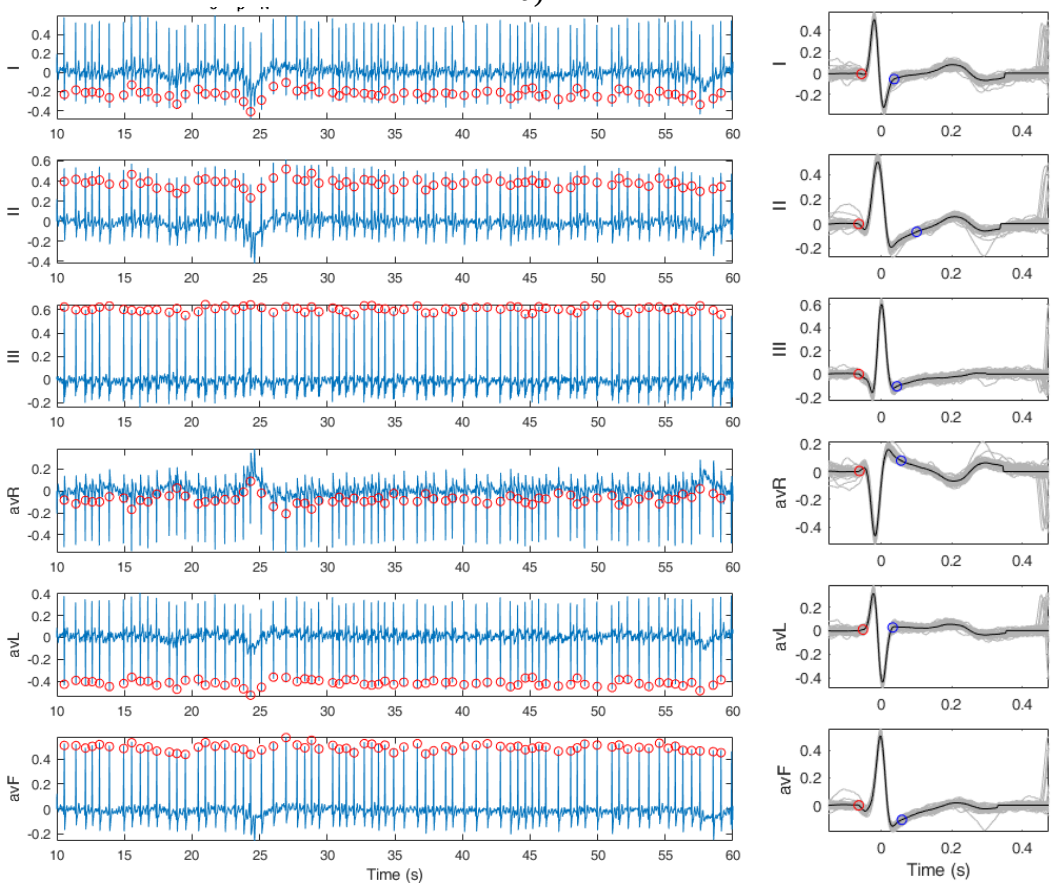
I
II
III
avR
avL
avF
Time (s)

b)

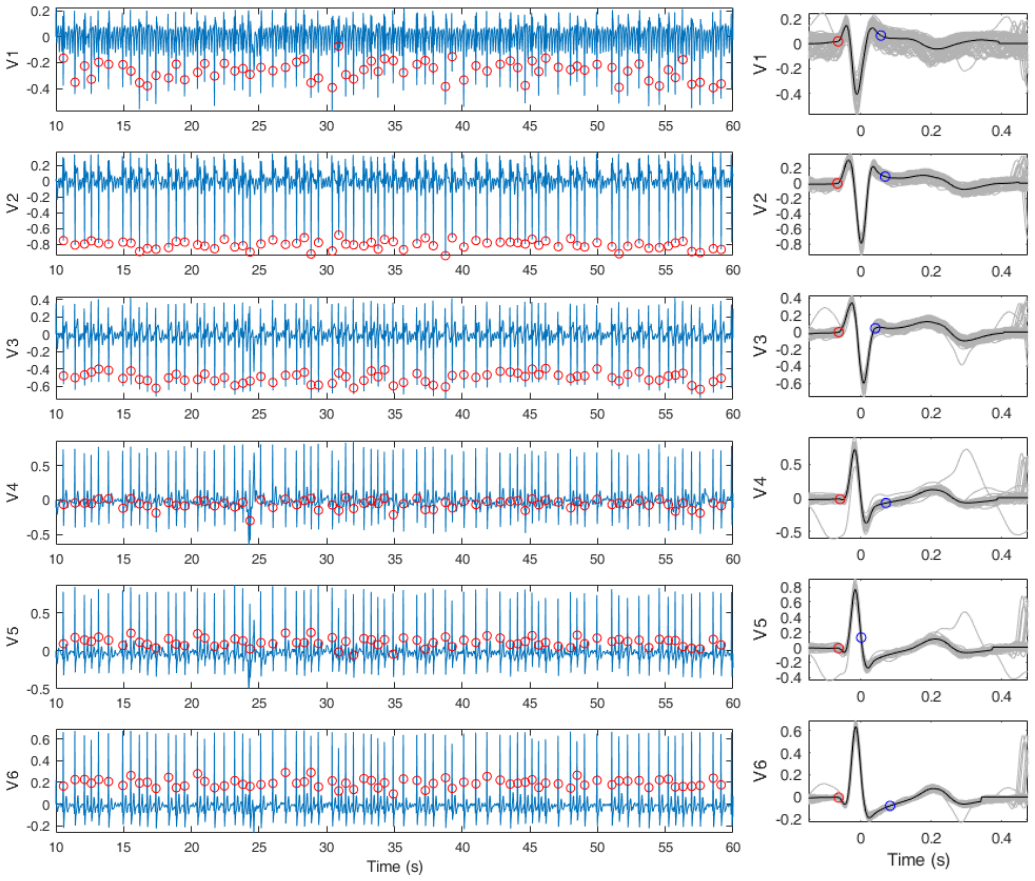

c)

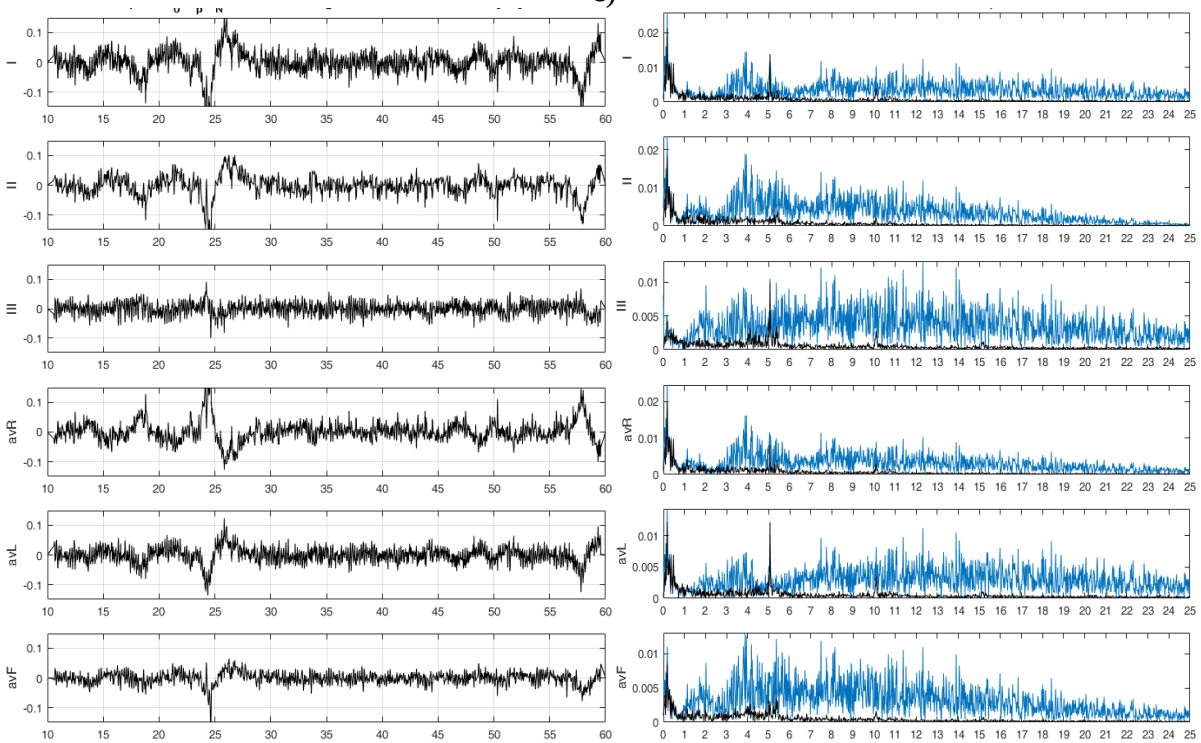

d)

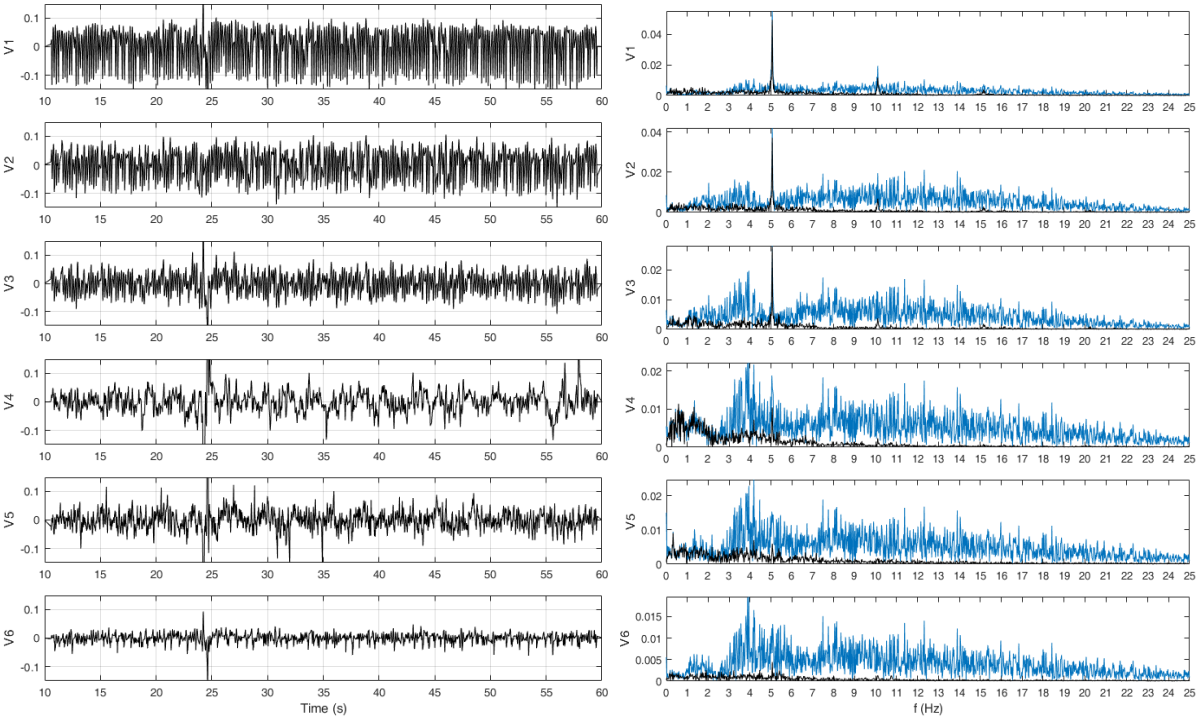

e)

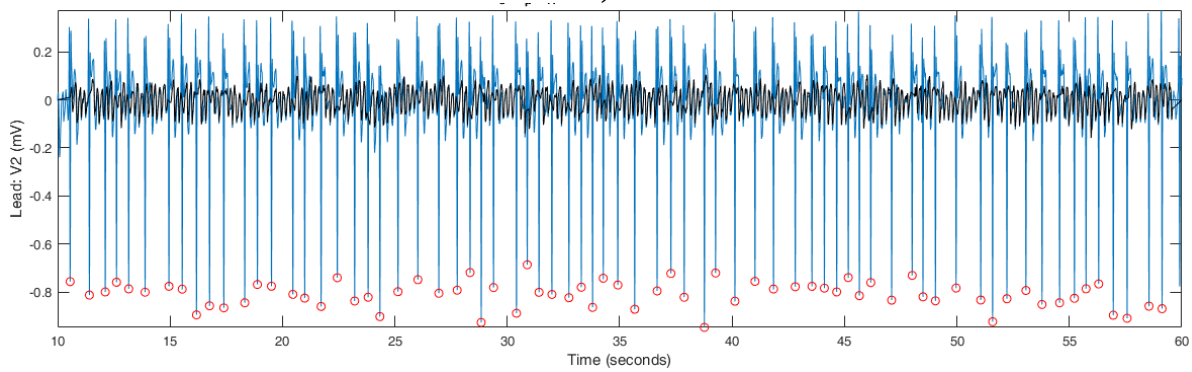

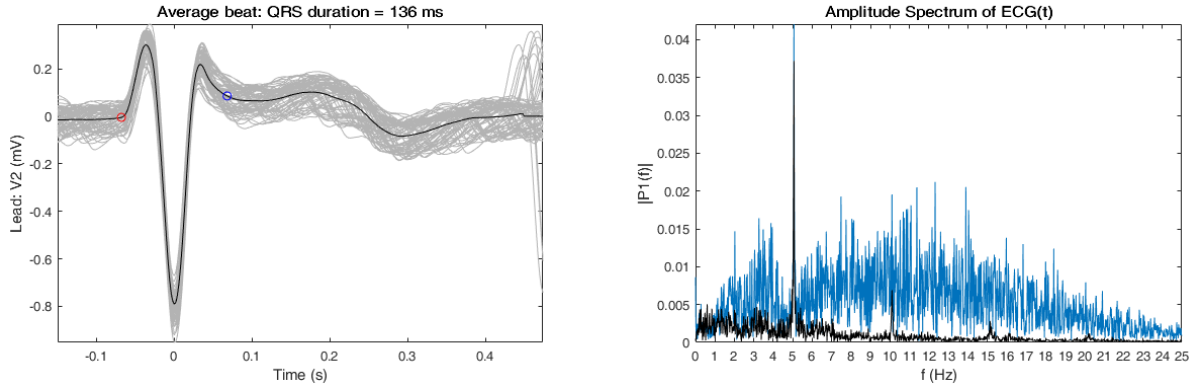

f)

Fig. 6 Sequential procedures for obtaining the amplitude-frequency spectrum by ECG registration for patient No. 10 of the AF relapse group postprocedurally: the original signal; the signal in the 12 leads with detected QRS-complex (left) and averaged QRS-complex in each lead; the signal after extraction of the averaged QRS-T segment; the amplitude-frequency spectra of the signal for each lead after extraction; the indicated procedures for the lead selected as representative lead V2.

As a result of the amplitude-frequency analysis of the f-waves in the two groups, we formed the following database of their morphological components for each patient:

Table 2. Spectral values – frequency and amplitude for each patient in both groups and number of f-waves per minute

	Patient No	**f-W-Hz**	**f-W-Ampl-mV**	**Nmbr-fW-pmin**	**Patient No**	**f-W-Hz**	**f-W-Ampl-mV**	**Nmbr-f-W-pmin**
1	1	4.3	0.0046	258	2	5	0.023	300
2	3	5.7	0.0048	342	6	6	0.005	360
3	4	7	0.0043	420	8	3.7	0.0095	222
4	5	6	0.0063	360	10	5	0.038	300
5	7	4.3	0.009	258	15	3.6	0.015	216
6	9	5.2	0.016	312	19	6	0.0083	360
7	11	5.4	0.0054	320	22	4.5	0.019	270
8	12	7.7	0.0039	462	21	6.8	0.0035	408
9	13	4.5	0.0048	270	25	6	0.009	360
10	14	5	0.0046	300	26	6	0.0035	360
11	16	5.5	0.0057	330	27	5.9	0.0048	354
12	17	5.1	0.0045	306	29	4.4	0.0128	264
13	18	5	0.0077	300	31	5.9	0.058	354
14	20	5.3	0.0056	319	33	5	0.004	300
15	23	5.2	0.0046	312				
16	24	5.5	0.0065	330				
17	28	5.3	0.0027	318				
18	30	5.7	0.0048	342				
19	32	5.5	0.0028	330				
20	34	4.1	0.0047	246				
21	35	4.3	0.0069	258				
22	36	4.5	0.004	270				
23	37	6.7	0.008	402				
24	38	5.7	0.003	342				
25	39	5.3	0.0034	318				

The f-W-Ampl-mV values indicated in the table **were determined by measuring the maximum spectral amplitude in the amplitude-frequency spectrum of each patient.**

Tables 3 and 4 show the results of descriptive analysis of morphological f-wave indices for the group of patients without recurrence and with recurrence after CA, respectively.

Table 3. Descriptive analysis of morphological f-wave indices for the group of patients without relapse

Descriptive Statistics (Ampl(mV); f(Hz)) without recurrence					
	Valid N	**Mean**	**Minimum**	**Maximum**	**Std.Dev.**
f-W-Hz	25	5.3154	3.6000	7.7000	0.92809
f-W-Ampl-mV	25	0.0054	0.0013	0.0160	0.00304
Nmbr-fW-pmin	25	318.9231	216.0000	462.0000	55.68549

Table 4. Descriptive analysis of morphological f-wave indices for the group of patients with relapse

Descriptive Statistics (Ampl(mV); f(Hz)) with recurrence					
	Valid N	**Mean**	**Minimum**	**Maximum**	**Std.Dev.**
f-W-Hz	14	5.2000	3.5000	6.8000	1.17047
f-W-Ampl-mV	14	0.0327	0.0045	0.0950	0.03413
Nmbr-f-W-pmin	14	310.3333	210.0000	408.0000	70.72482

The histograms of the distribution of the f-wave amplitudes in patients without AF recurrence after ablation and patients with AF recurrence are shown in Figs. 7 and 8, respectively. The red line indicates the theoretical normal distribution of the statistical estimates for the two distributions, respectively, as determined by the Kolmogorov-Smirnov test.

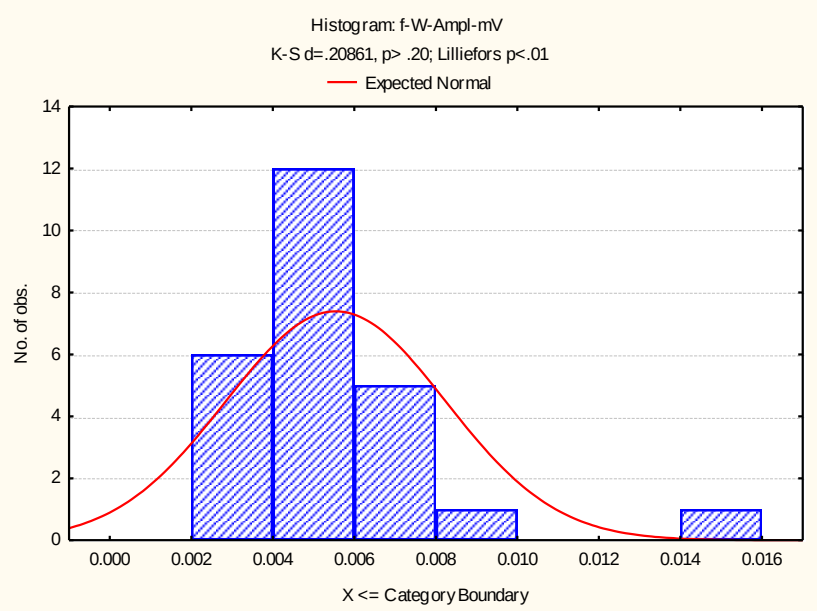

Fig. 7 No recurrence – distribution of values close to normal centered between 0.002 and 0.008 mV – overall, there were 23 cases out of 25, or 92% of cases, in this low-voltage interval

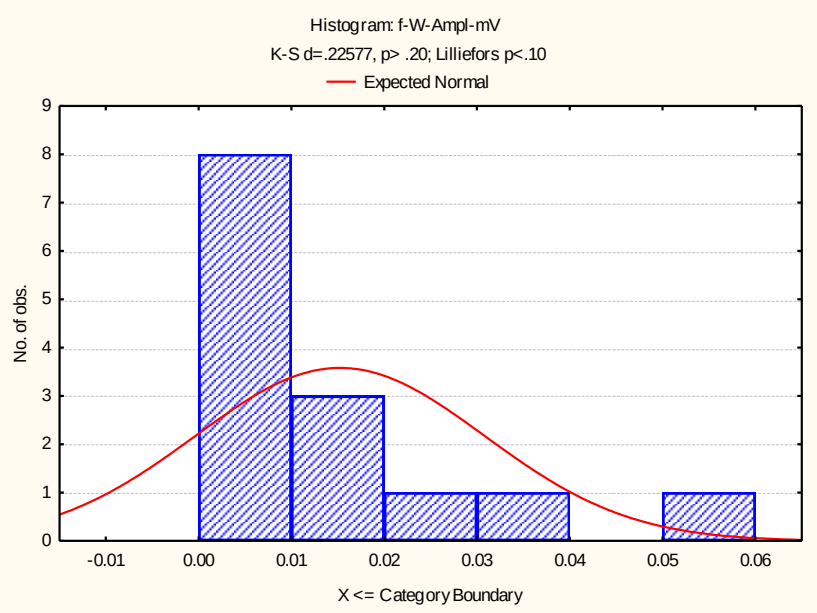

Fig. 8 With recurrence – distribution of values with high asymmetry towards the higher values 0.1-0.2 mV – 11 cases of 14, or 79% of cases

For the f-W-Hz frequency metric, there is a certain feature: there is a pronounced clustering of values in the relapse group towards higher frequency (Fig. 9).

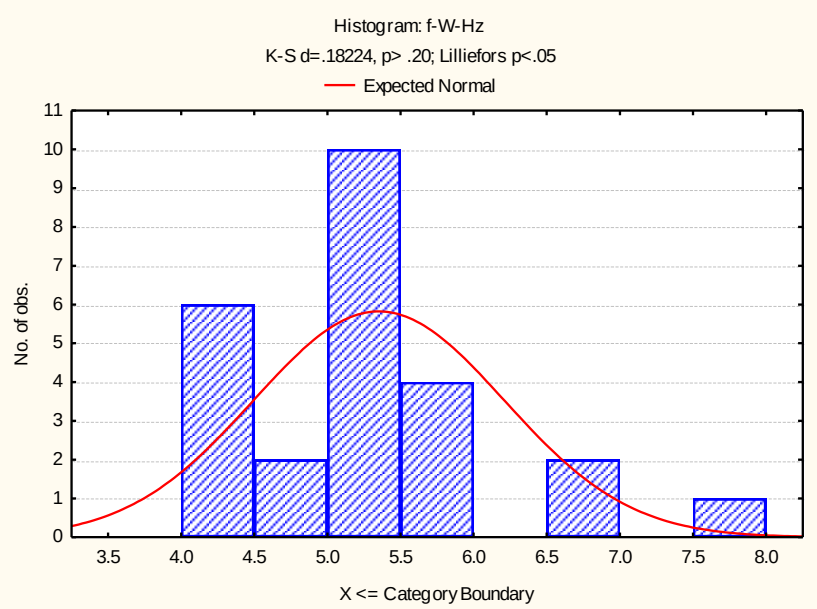

Fig. 9 Distribution of frequency index values in the group without relapse

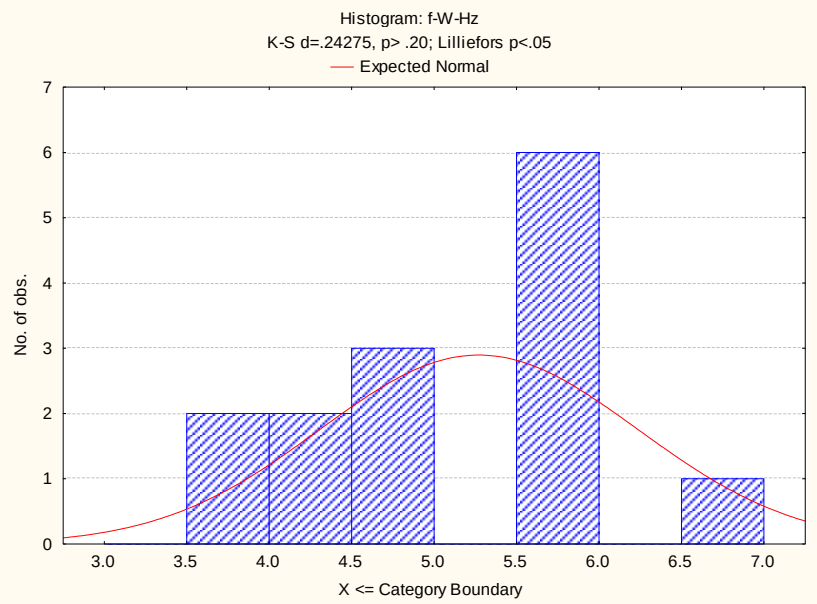

Fig. 10 Distribution of frequency index values in the relapse group

Apparently, the distribution of values for the amplitudes and frequencies of the f-waves in patients with relapse differed significantly from normal. Because of this, and because of the small and different number of patients in the two study groups, we used the Mann-Whitney test to assess the significance of the differences in these parameters between the two groups - the results are given in Table 5 (in the table a significant difference with $p < 0.05$ is marked in red).

Table 5. U-test for differences between amplitude and frequency indices in the groups without and with AF relapse

variable	Mann-Whitney U Test (categor-U) By variable categor Marked tests are significant at p <.05000							
	U	Z	p-level	Z adjusted	p-level	Valid N Group 1	Valid N Group 2	2*1sided exact p
f-W-Hz	169.0000	-0.17566	0.860560	-0.17622	0.860125	25	14	0.873712
f-W-Ampl-mV	89.5000	-2.50318	0.012309	-2.50534	0.012234	25	14	0.010997

The result of the test showed a significant difference between the amplitude values in the two groups of patients.

Selection of indicators for classification of groups of patients with and without recurrences of AF in the postoperative period.

Our stepwise discriminant analysis identified, out of 14 metrics (columns 1 to 13 in Table 1, and the amplitude of the f-waves), 5 that reliably separated the groups without and with relapse.

The numerical values obtained for the statistics in Table 6 are Echo LV-EF, f-W-Ampl, HF, Stroke/TIA, Diab. The contribution of these indices to the total score was (in the order indicated) 27.2%, 3.62%, 2.62%, 14.4%, 12.2%, respectively.

Table 6. Summary values of the stepwise discriminant analysis results for the determined indicators with reliable classification ability

Discriminant Function Analysis Summary (Epicrisa + Fa-f) Step 5, *N* of vars in model: 5; Grouping: no-sas (2 grps); Wilks' Lambda: 0.38526 approx. $F = 7.0208$; $p < 0.0005$						
	Wilks' Lambda	**Partial Lambda**	***F*-remove**	***p*-level**	**Toler.**	**1-Tolerance (R^2)**
Echo LV-EF	0.722417	0.533296	19.25293	0.000234	0.413442	0.586558
HF	0.665234	0.579137	15.98757	0.000605	0.454221	0.545779
f-W-Ampl-mV	0.678300	0.567981	16.73372	0.000483	0.263223	0.736777
Stroke/TIA	0.562286	0.685170	10.10883	0.004337	0.282336	0.717665
Diab.	0.535465	0.719489	8.57725	0.007775	0.608372	0.391628

The parameter with the highest contribution to discrimination between the two groups was the left ventricular ejection fraction (Echo LV-EF). What is significant in this case, for the purposes of our study, is the involvement of the spectral amplitude index of f-waves, with the second most important contribution to the discrimination between the two groups of patients, whereby we have reason to accept the prognostic significance of f-wave morphology for AF recurrence after ablation. The result for the multiple correlation (R^2) between the f-wave amplitude index and the other indices involved in discrimination is also interesting, with the highest correlation for this index.

The two linear discriminators corresponding to the two groups of patients have, respectively, coefficients in front of the indices shown in Table 7.

Table 7. Coefficients in front of the determined indices in the two discriminators

Classification functions; grouping: with-without (Epicrisis + f-Ampl)		
	G_1:1	**G_2:2**
Echo LV-EF	2.2092	2.6402
HF	64.0511	80.4150
f-W-Ampl-mV	71.5914	94.8619
Stroke/TIA	-40.8812	-53.4644
Diab	15.6166	21.1570
Constant	-62.5339	-90.3506

In linear form, the discriminators look like this (with rounding to hundredths):

G_1 = 2.21*Echo LV-EF + 64.05*HF + 71.59*f-W-Ampl-mV – 40.88*Stroke/TIA + + 15.62*Diab – 62.53

G_2 = 2.64*Echo LV-EF + 80.4 2*HF + 94.86*f-W-Ampl-mV – 53.46*Stroke/TIA + + 21.16*Diab – 90.35

The assignment of a specific patient to one of the two groups is performed by substituting his values for the 5 indicators into the linear discriminators and if the resulting number is greater for the 1st discriminator, the patient is assigned to the 1st group (in the case without postprocedural AF relapse), if the resulting number is greater for the 2nd discriminator – the assignment is to the 2nd group (with postprocedural AF relapse).

To facilitate classification, we used a decision rule based on the difference between the two linear discriminators **G_1 – G_2**, keeping in mind that for a given patient's data, if G_1 has a larger value than G_2, the difference is positive and the patient is assigned to the group without relapse; if G_2 has a larger value than G_1, the difference is negative and the patient is assigned to the group with relapse. In this case

G_1 – G_2 = –0.43*(Echo LV-EF) – 16.36*HF – 23.27* (f-W-Ampl) +
+ 12.58*Stroke/TIA – 5.54*Diab + 27.82,

which is the decisive classification rule.

The last column of Table 8 shows the difference between G_1 and G_2, with positive values assigning the patient to the group without relapse and negative values to those with relapse.

A visual representation of the distribution of the values of the decision rule by patient data in the group without recurrence and in the group with AF recurrence postprocedurally, is given by Figs. 11 and 12, respectively.

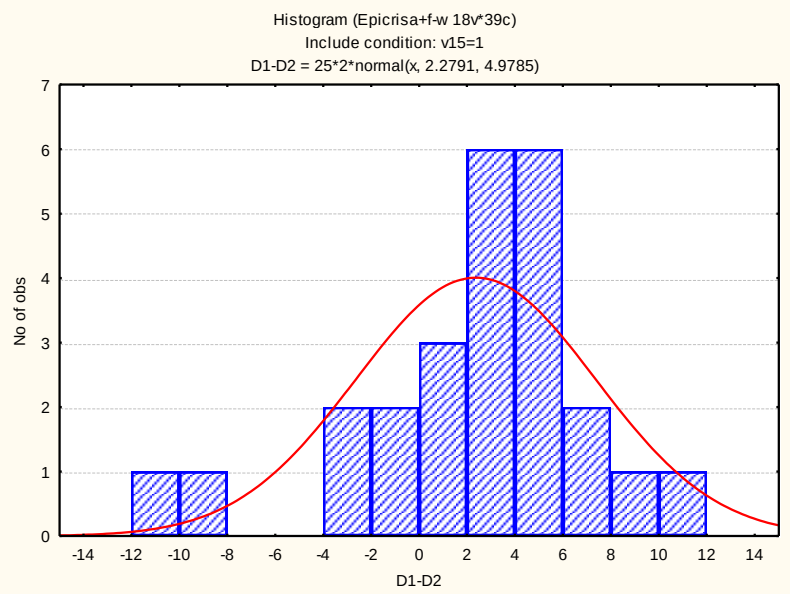

Fig. 11 Distribution of values for the decision rule – relapse-free group

Table 8. Values for the decision rule for each patient in the two groups (marked with 1 and 2 in column16, respectively). Misclassified patients are marked in red.

	Age	Height	Weight	BMI	Hx of AF yrs	Hypert	Diab	Stroke / TIA	HF	CHD	CHADsV asc score	Echo LA diam	Echo LV-EF	f-W-Ampl-mV	With / without	G_1 -G_2
1	54	190	120	33	3	0	0	0	0	0	0	47	42	0.0046	1	9.61
2	67	190	110	30	1	1	0	0	0	0	2	43	54	0.023	2	4.01
3	44	190	124	34	5	1	0	0	0	0	1	42	51	0.0054	1	5.51
4	67				1	1	1	1	0	0	5	60	56	0.0043	1	10.62
5	67	176	86	28	3	1	1	0	1	1	5	49	33	0.0063	1	-8.46
6	57	176	110	35	11	1	0	0	0	0	1	44	65	0.005	2	-0.31
7	57	183	97	29	25	1	0	0	0	0	1	40	70	0.009	1	-2.56
8	58	170	90	31	2	1	1	0	0	0	2	50	61	0.0095	2	-4.24
9	61	176	107	35	2	1	0	0	0	0	1	44	55	0.016	1	3.74
10	58	186	90	26	1	1	0	0	0	0	1	47	70	0.038	2	-3.24
11	60	160	85	33	8	1	0	0	0	0	2	38	52	0.0054	1	5.28
12	48	185	90	26	2	0	0	0	0	0	0	42	59	0.0039	1	2.30
13	66	176	90	29	9	1	1	1	0	0	5	47	68	0.0048	1	5.44
14	66	170	93	32	4	1	0	0	0	0	2	43	67	0.0046	1	1.17
15	58	177	137	44	12	1	1	0	0	0	2	56	62	0.015	2	-4.79
16	68	178	78	25	1	1	0	0	0	0	2	45	55	0.0057	1	3.98
17	72	183	100	30	2	1	0	0	0	1	3	43	63	0.0045	1	0.56
18	54	180	120	37	3	1	0	0	0	0	1	60	54	0.0077	1	4.36
19	63	164	97	36	5	1	1	0	0	0	3	40	61	0.0083	2	-4.21
20	58	163	63	24	2	1	0	0	0	0	2	45	61	0.0054	1	1.40
21	71	173	84	28	1	1	0	1	1	0	4	54	54	0.0035	2	-0.68
22	53	179	71	22	6	0	0	0	0	0	0	45	62	0.019	2	-0.65
23	64					1	0	0	1	0	2	38	53	0.0046	1	-11.50
24	70	172	75	25	1	0	0	0	0	0	2	40	50	0.0065	1	6.12
25	58	170	80	28	1	1	0	0	0	0	2	40	65	0.0035	2	-0.28
26	53	180	82	25	1	0	0	1	0	0	2	35	55	0.95	2	-5.41
27	65	173	100	33	2	1	0	0	1	1	4	50	38	0.0048	2	-5.04
28	64	175	112	37	10	1	0	0	0	0	1	48	65	0.0027	1	0.26
29	66	171	88	30	15	1	0	0	0	0	3	45	68	0.0128	2	-1.79
30	51	180	90	28	1	1	0	0	0	0	1	43	50	0.0048	1	6.16
31	63	172	70	24	1	1	0	0	0	0	1	40	61	0.058	2	-0.18
32	74	170	70	25	2	1	1	0	0	1	4	44	45	0.0028	1	2.82
33	52	185	88	26	1	1	0	0	0	0	1	43	65	0.004	2	-0.29
34	60	179	90	28	3	1	0	0	0	1	2	42	54	0.0047	1	4.43
35	65	163	63	24	2	1	0	0	0	0	3	44	61	0.0069	1	1.37
36	72	163	92	34	3	1	0	0	0	0	3	43	52	0.004	1	5.31
37	55	180	90	27	4	0	0	0	0	0	0	40	59	0.008	1	2.20
38	58	176	118	38	3	1	0	0	0	1	1	44	57	0.003	1	3.18
39	64	165			4	1	1	0	0	0	1	44	60	0.0034	1	3.66

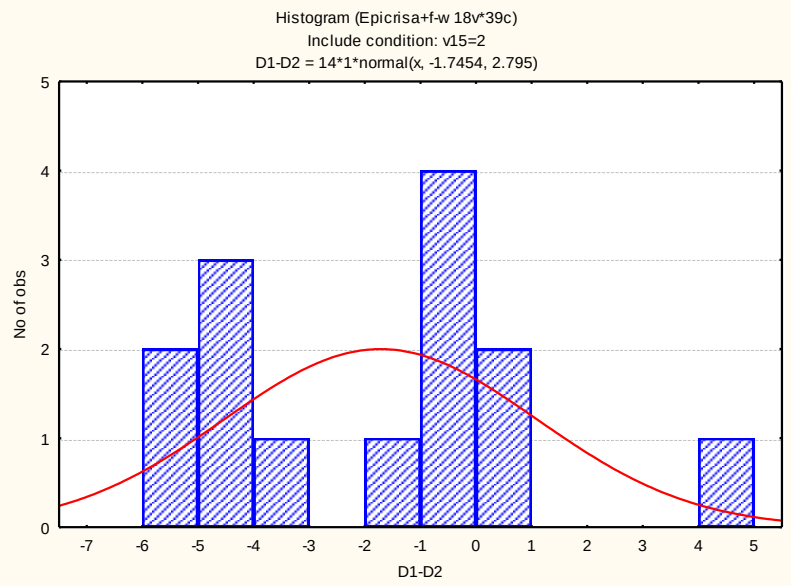

Fig. 12 Distribution of values for the decision rule – relapse group

Hypothesis for possible synthesis of a model for prediction of postprocedural AF recurrences after catheter ablation using data from the preprocedural period

Following the results obtained in the previous sections – a significant difference between the spectral amplitudes of f-waves in the two groups of patients – with and without AF recurrence after CA, as well as the significant involvement of spectral amplitudes in constellation with indicators of comorbidities and ultrasound imaging, we undertook to verify the feasibility of developing a model to predict postprocedural AF recurrence after CA. **The main aim and application of discriminant analysis point towards such a hypothesis: to use the model to classify new subjects to one of the study populations (groups).**

The decision rule synthesized on the available data classified, among the 39 patients, 25 without relapse (group 1) and 14 with relapse (group 2), 3 patients erroneously from group 1 to group 2 (false positive), or 12%, and 1 patient erroneously from group 2 to group 1 (false negative), or 7.1%. This result was achieved based on the 5 parameters that reliably separate the two groups: Echo LV-EF, f-W-Ampl, HF, Stroke/TIA, Diab. The Sensitivity, Specificity and Accuracy of the decision rule were respectively:

Sensitivity = 22/(22 + 1) = 0.96, or 96%;

Specificity = 13/(13 + 3) = 0.813, or 81.3%;

Accuracy = 1 – (4/39) = 0.897, or 89.7%.

Returning to the distributions of the values of the decision rule for the two groups of patients studied (Figs. 11 and 12), we can determine a cutoff value to determine the risk of recurrence after ablation in the patients studied:

- **a value of G_1 – G_2 > 0 implies a low risk of relapse;**
- **a value of G_1 – G_2 ≤ 0 implies a high risk of relapse.**

These results provide a basis to hypothesize that it is possible to develop an algorithm (decision rule) for determining the degree of risk of postprocedural AF recurrence from data from the preprocedural period. We will recall the main requirement for realizing this possibility: it is correct to apply the DA model (decision rule) to new patients after it has been approximated on data of patients not included in the training groups (samples) during rule synthesis, and thus to have determined the real sensitivity and specificity of the model, i.e. to use the procedure for classification of future items (patients) after the procedure has been verified on independent items.

Another condition supporting the applicability of the DA model is to increase the number of items in the training samples to a level that leads to higher reliability of discrimination statistics.

Under these conditions, the hypothesis for the development of a discriminant model for the determination of the risk of recurrence of AF after catheter ablation will lead to a practical and convenient for use in clinical settings algorithm for pre-procedural scoring (numerical) risk assessment, including by risk levels – low, moderate and high.

Discussion and conclusion

Despite the significant progress in the success rate of interventional treatment in AF, a significant proportion of patients still exhibit arrhythmia recurrence after the procedure. The search for possible predictors of procedural success is of utmost importance to improve its effectiveness and better patient selection.

In addition to standard clinical indices serving as predictors of AF episodes after ablation [1], more attention has been paid in recent years to potential ECG characteristics of fibrillatory waves. In our work, ECG parameters alone did not reach a high predictive value for recognizing patients at risk of AF recurrence after ablation. Similar results have been reported in the past. In a publication, Chang et al. [2] reported that the dominant frequency, as a single indicator, was not sufficient to reach a statistically significant predictive value for a recurrence-free period after ablation. This changes when more than one ECG parameter is added to the calculation.

One of the main practical benefits of the present work is the synthesis of a quantitative algorithm, incorporating echocardiographic, clinical, and ECG data, thus arriving at a crucial rule allowing the preprocedural assessment of the risk of AF recurrence. By incorporating into the algorithm a comprehensive assessment that brings together the echographic index of left ventricular ejection fraction, heart failure and two clinical indicators, diabetes mellitus and ischemic stroke, as well as the ECG index of f-wave amplitude, it is possible to more fully assess the risk of recurrence in a given patient.

In our study, we assumed that the combination of instrumental and clinical parameters would provide a high predictive value, and in the follow-up, we reported the parameters providing the highest predictive value. The parameter with the highest contribution to discrimination between the two groups (those with relapse and those without relapse) was left ventricular ejection fraction (Echo LV-EF). To date, there is no definitive literature evidence for a specific threshold of Echo LV-EF, below which the probability of AF recurrence after CA increases, but the association between reduced ejection fraction and poor prognosis is known and demonstrated in a number of publications and meta-analyses [1, 10]. Despite the high

contribution in the scoring system, differences in EF values alone do not indicate a sufficiently high predictive ability.

What is significant in this case, for the purposes of our study, is the involvement of the spectral amplitude index of the f-waves, with a second more important contribution to the discrimination between the two groups of patients, whereby we have reason to accept the prognostic significance of f-wave morphology for AF recurrence after ablation. Several publications have reported the importance of f-wave amplitude as a predictor of arrhythmia duration, or as a predictor of intraprocedural arrhythmia termination in patients with persistent AF, as well as of sinus rhythm maintenance at 12-month follow-up [15, 23].

To increase sensitivity, some authors have proposed algorithms for automatic amplitude readout and the use of more than one lead [23]. Particularly interesting is the result for the multiple correlation between the spectral amplitude index of f-waves and the other indices involved in discrimination, with the highest correlation for this index. To date, the literature lacks an algorithm for determining the risk of AF recurrence that incorporates the predictive ability of the spectral amplitude of f-waves combined with clinical indicators, and this is one of the main practical benefits. A similar approach of combined analysis of ECG parameters coupled with clinical indicators has been reported by Matsuo et al. [11], but in that work the AF cycle measured manually on a surface ECG was reported, combined with intracardiac parameters from the left atrial and right atrial auricles, and the f-wave amplitude was not investigated. Another significant difference of our work, compared to the previous publication, is that the approach is entirely noninvasive, allowing the calculation of the probability of recurrence before ablation is performed.

Concomitant diabetes mellitus has been described as a risk factor for the development of AF [21], but data on ischaemic stroke are scarce. It is likely that the presence of AF is an indicator of a long-standing arrhythmia in which optimal medical control has not been applied, and ischemic stroke (IS) itself is a manifestation of this. The CRYSTAL-AF study described detection of AF in 30% of patients with AMI or transient ischaemic attack by the third year of the event, perhaps confirming that atrial fibrillation accompanies some patients long before its diagnosis [17].

Another important practical relevance, is that the added ECG recording and analysis, as well as the proposed hypothesis for determining the risk of postprocedural AF recurrences (after its verification), are fully compatible with the algorithm of work in most clinics, do not prolong the patient's stay and do not bring additional risk to his health.

A major limitation of any quantitative system for the prediction of AF recurrence is the complex pathogenesis of this arrhythmia, involving triggers with high-frequency activity and a pathological substrate in the atria, capable of sustaining the arrhythmia, and ablation would be differentially effective for different mechanisms of the arrhythmia. Another possible limitation could be the multiple variable parameters during a complex and complicated procedure, such as AF ablation, such as lesion continuity around the pulmonary veins and/or linear lesions in the atrium. This in turn can lead to a difficult to prognosticate long-term outcome of the procedure and makes the creation of a high-fidelity risk score very difficult. It is these variables that are a possible cause of the 4 misreported cases in our paper.

Acknowledgement

This work has been partially supported by the Bulgarian National Science Fund, Grant No KP-06-H42/3.

References

1. Balk E. M., A. C. Garlitski, A. A. Alsheikh-Ali, T. Terasawa, M. Chung, S. Ip (2010). Predictors of Atrial Fibrillation Recurrence after Radiofrequency Catheter Ablation: A Systematic Review, J Cardiovasc Electrophysiol, 21(11), 1208-1216.
2. Chang S.-H., M. Ulfarsson, A. Chugh, et al. (2011). Time- and Frequency-domain Characteristics of Atrial Electrograms during Sinus Rhythm and Atrial Fibrillation, J Cardiovasc Electrophysiol, 22(8), 851-857.
3. Chen S., B. Schmidt, S. Bordignon, et al. (2019). Ablation Index-guided 50 W Ablation for Pulmonary Vein Isolation in Patients with Atrial Fibrillation: Procedural Data, Lesion Analysis, and Initial Results from the FAFA AI High Power Study, J Cardiovasc Electrophysiol, 30, 2724-2731, https://doi.org/10.1111/jce.14219.
4. Cheng Z., H. Deng, K. Cheng, et al. (2013). The Amplitude of Fibrillatory Waves on Leads aVF and V1 Predicting the Recurrence of Persistent Atrial Fibrillation Patients Who Underwent Catheter Ablation, Ann Noninvasive Electrocardiol, 18(4), 352-358.
5. Christov I., I. Simova (2006). Fully Automated Method for QT Interval Measurement in ECG, Computers in Cardiology, 33, 321-324.
6. Hindricks G., T. Potpara, N. Dagres, et al. (2021). ESC Scientific Document Group, European Heart Journal, 42(5), 373-498, doi: 10.1093/eurheartj/ehaa612.
7. IEC 60601-2-25:2011 Medical Electrical Equipment – Part 2-25: Particular Requirements for the Basic Safety and Essential Performance of Electrocardiographs.
8. Kirchhof P., S. Benussi, D. Kotecha, et al. (2016). 2016 ESC Guidelines for the Management of Atrial Fibrillation Developed in Collaboration with EACTS, European Heart Journal, 37(38), 2893-2962, https://doi.org/10.1093/eurheartj/ehw210.
9. Kuhn M., K. Johnson (2013). Discriminant Analysis and Other Linear Classification Models, In: Applied Predictive Modeling, Springer, New York, NY, https://doi.org/10.1007/978-1-4614-6849-3_12.
10. Liżewska-Springer A., A. Dąbrowska-Kugacka, E. Lewicka, et al. (2020). Echocardiographic Predictors of Atrial Fibrillation Recurrence after Catheter Ablation: A Literature Review, Cardiol J, 27(6), 848-856, doi: 10.5603/CJ.a2018.0067.
11. Matsuo S., N. Lellouche, M. Wright, et al. (2009). Clinical Predictors of Termination and Clinical Outcome of Catheter Ablation for Persistent Atrial Fibrillation, J Am Coll Cardiol, 54(9), 788-795.
12. McManus D. D., M. Rienstra, E. J. Benjamin (2012). An Update on the Prognosis of Patients with Atrial Fibrillation, Circulation, 126(10), e143-e146.
13. Nault I., N. Lellouche, S. Matsuo, et al. (2009). Clinical Value of Fibrillatory Wave Amplitude on Surface ECG in Patients with Persistent Atrial Fibrillation, J Interv Card Electrophysiol, 26(1), 11-19, doi: 10.1007/s10840-009-9398-3.
14. Packer D. L., D. B. Mark, R. A. Robb, et al. (2019). Effect of Catheter Ablation vs Antiarrhythmic Drug Therapy on Mortality, Stroke, Bleeding, and Cardiac Arrest among Patients with Atrial Fibrillation: The CABANA Randomized Clinical Trial, JAMA, 321(13), 1261-1274, doi: 10.1001/jama.2019.0693.
15. Park J., C. Lee, E. Leshem, et al. (2019). Early Differentiation of Long-standing Persistent Atrial Fibrillation Using the Characteristics of Fibrillatory Waves in Surface ECG Multi-leads, Sci Rep, 9(1), 2746, doi: 10.1038/s41598-019-38928-6.
16. Petrovski P. (2017). Atrial Fibrillation, Sahakhari Stoyanov Publ, Sofia, (in Bulgarian).

17. Sanna T., H.-C. Diener, R. S. Passman, et al. (2014). Cryptogenic Stroke and Underlying Atrial Fibrillation, New England Journal of Medicine, 370(26), 2478-2486.
18. Shimamoto K., F.Miura, Y. Shimatani, et al. (2018). Pulmonary Vein Volume Predicts the Outcome of Radiofrequency Catheter Ablation of Paroxysmal Atrial Fibrillation, PLoS ONE, 13(7), e0201199, https://doi.org/10.1371/journal.pone.0201199.
19. Stoyanov T. (2019-2020). Computer Based ECG System, Annual of the Informatics Section, Union of Scientists in Bulgaria, 10, 55-62 (in Bulgarian).
20. Sultan A., J. Lüker, D. Andresen, et al. (2017). Predictors of Atrial Fibrillation Recurrence after Catheter Ablation: Data from the German Ablation Registry, Sci Rep, 7(1), 16678, doi: 10.1038/s41598-017-16938-6.
21. Sun Y., D. Hu (2010). The Link between Diabetes and Atrial Fibrillation: Cause or Correlation?, Journal of Cardiovascular Disease Research, 1(1), 10-11.
22. Tabakov S., I. Iliev, V. Krasteva (2008). Online Digital Filter and QRS Detector Applicable in Low Resource ECG Monitoring Systems, Annals of Biomedical Engineering, 36(11), 1805-1815, doi: 10.1007/s10439-008-9553-5.
23. Zarzoso V., D. G. Latcu, A. R. Hidalgo-Muñoz, et al. (2016). Non-invasive Prediction of Catheter Ablation Outcome in Persistent Atrial Fibrillation by Fibrillatory Wave Amplitude Computation in Multiple Electrocardiogram Leads, Archives of Cardiovascular Diseases, 109(12), 679-688, https://doi.org/10.1016/j.acvd.2016.03.002.

Iskren Garvanski, M.D., Ph.D. Student
E-mail: i.garvanski@gmail.com

Dr. Iskren Garvanski graduated in Medicine at the Medical University – Sofia in 2013. In 2019 he acquired a degree in Cardiology. He holds EHRA Certification in Electrophysiology (2021), Certificate of Pacemaking – expert level (2021), EHRA Certification in Cardiac Device Specialist (2020), and Certificate of Echocardiography – fundamental level (2020). Since 2019 he has been a cardiologist in the Department of Cardiology and Electrophysiology, University Adcibadem City Clinic Ltd, Sofia. Currently, he is a Ph.D. Student at the Institute of Biophysics and Biomedical Engineering – BAS.

Prof. Mikhail Matveev, Ph.D., FESC
E-mail: mgm@biomed.bas.bg

Professor of Biomedical Engineering Mikhail Matveev holds the degrees of M.Sc. in Nuclear Physics, Computing Mathematics and Ph.D. in area of Medicine. His publications are in the fields of biomedical engineering in cardiovascular diseases and electrocardiology, neurology, resuscitation and intensive care, emergency medicine, pulmonary diseases, methods for optimization of the diagnostic and therapeutic process, autonomic cardiac control, information technologies in medicine etc. Prof. Matveev is a winner of many national and international awards, he is an honorary innovator, an excellent student of the Ministry of Health, an honorary member of the Union of Scientists in Bulgaria.

Prof. Vessela Krasteva, Ph.D.
E-mail: vessika@biomed.bas.bg

Vessela Krasteva holds a M.Sc. degree in Electronic Engineering from the Technical University – Sofia (1998) and a Ph.D. degree in Biomedical Engineering (2001). Since 2018, she is a Professor and Head of the Department "Analysis and Processing of Biomedical Signals and Data" at the Institute of Biophysics and Biomedical Engineering, Bulgarian Academy of Sciences. Prof. Krasteva is a co-author of more than 100 peer review journal papers in the field of machine learning, signal processing and electrocardiology. Her main research interests are permanently focused on improving treatment of out-of-hospital cardiac arrest; development of algorithms for processing and measurement of electrocardiographic signals and data; computer aided diagnosis of cardiac pathologies based on machine learning and deep neural networks.

Senior Assist. Prof. Todor Stoyanov, Ph.D.
E-mail: tstoyanov72@gmail.com

Todor Stoyanov graduated as M.Sc. from the Faculty of Electronics, Technical University of Sofia, in 1999. Since 1999 he is with the Centre of Biomedical Engineering and the Institute of Biophysics and Biomedical Engineering, Bulgarian Academy of Sciences. He is a Senior Assistant Professor since 2002. He obtained Ph.D. degree in 2005 on Computer Aided Processing and Analysis of Electrocardiograms. His interests are in developing embedded systems for biomedical signal analysis.

Prof. Iana Simova, M.D., Ph.D.
E-mail: ianahr@ yahoo.com

Prof. Dr. Iana Simova, Ph.D., is a Head of the Cardiology Clinic at the Heart and Brain Center of Excellence, University Hospital Pleven. She graduated from the Medical University in Sofia. She specializes in Cardiology at the National Cardiology Hospital – Sofia, and in Italy, under the guidance of leading specialists in echocardiography. In 2015 she became an Associate Professor and in 2021 a Professor. Prof. Simova is a leading specialist in echocardiography in Bulgaria. She has held senior positions, including in the European Society of Cardiology and the European Association of Cardiovascular Imaging.